Multifunctional "Hydrogel Skins" on Diverse Polymers with Arbitrary Shapes

DOI: 10.1002/((please add manuscript number))

Article type: Communication

Multifunctional "Hydrogel Skins" on Diverse Polymers with Arbitrary Shapes

Yan Yu[#], Hyunwoo Yuk[#], German A. Parada[#], You Wu, Xinyue Liu, Christoph S. Nabzdyk, Kamal Youcef-Toumi, Jianfeng Zang, Xuanhe Zhao[*]

Dr. Y. Yu, H. Yuk, G. A. Parada, Dr. Y. Wu, X. Liu, Prof. K. Youcef-Toumi, Prof. X. Zhao

Department of Mechanical Engineering, Massachusetts Institute of Technology, Cambridge, MA 02139, USA

*E-mail: zhaox@mit.edu

Dr. Y. Yu, Prof. J. Zang

School of Optical and Electronic Information, and Innovation Institute, Huazhong University of Science and Technology, Wuhan 430074, China

Dr. C. S. Nabzdyk

Department of Anesthesiology, Critical Care and Pain Medicine, Massachusetts General Hospital, Harvard Medical School, Boston, MA 02115, USA

Dr. C. S. Nabzdyk

Department of Anesthesiology and Perioperative Medicine, Mayo Clinic, Rochester, MN 55905, USA

Prof. X. Zhao

Department of Civil and Environmental Engineering, Massachusetts Institute of Technology, Cambridge, MA 02139, USA

#These authors contributed equally to this work.

Keywords: Hydrogels, Polymer devices, Coatings, Low friction, Antifouling, Biomedical devices

Abstract

Soft, slippery, and hydrophilic surfaces find critical applications in areas as diverse as biomedical devices, microfluidics, antifouling, and underwater robots. Existing methods to achieve such surfaces rely mostly on grafting hydrophilic polymer brushes or coating hydrogel layers, but these methods suffer from several limitations. Grafted polymer brushes are prone to damage and don't provide sufficient mechanical compliance due to their nanometer-scale thickness. Hydrogel coatings are applicable only for relatively simple geometries, precluding their use for the surfaces with complex geometries and features. Here, we propose a new method to interpenetrate hydrophilic polymers into the surface of diverse polymers with arbitrary shapes to form naturally integrated "Hydrogel Skins". The hydrogel skins exhibit tissue-like softness (Young's modulus ~ 30 kPa), have uniform and tunable thickness in the range of 5 to 25 μm, and can withstand prolonged shearing forces with no measurable damage. The hydrogel skins also provide superior low-friction, antifouling, and ionically conductive surfaces to the polymer substrates without compromising their original mechanical properties and geometry. We further demonstrate applications of the hydrogel skins on inner and

outer surfaces of various practical polymer devices including medical tubing, Foley catheters, cardiac pacemaker leads, and soft robots on massive scales.

Polymer-based devices with complex geometry are ubiquitous in a wide range of areas including bioengineering,[1] medical and clinical devices,[2,3] microfluidics,[4] and soft robotics.[5,6] In many applications, these polymer devices are used in close contact with human body. For instance, the intravenous delivery of therapeutic fluids, a routine procedure for hospitalized patients, is accomplished by using different types of vascular catheters.[7] Moreover, soft robotic devices such as heart sleeves[8] and drug delivery reservoirs[9] have been recently proposed as surgically-implantable devices. However, the majority of polymers used in these devices (e.g., polypropylene, polyethylene, polyvinyl chloride, polyurethane, silicone rubbers, and natural rubbers) have much higher elastic moduli (e.g., Young's modulus of 1 MPa to 1 GPa) than that of soft tissues in human body (e.g., Young's modulus of 1 to 100 kPa).[10,11] This stark mismatch in mechanical properties, coupled with the lack of bio-functionality, gives rise to numerous issues and complications during their clinical use such as tissue trauma, bio-fouling, thrombosis, and foreign-body reaction.[1,2,12-17] To address these shortcomings, it is necessary to modify the device surfaces to better match the properties of biological tissues.[2,13,18]

The most common strategy for surface modification involves grafting hydrophilic polymer chains (such as poly-N-vinylpyrolidone or polyethylene oxide/glycol) to the polymeric surfaces.[17,19-21] The resulting surfaces are hydrophilic and lubricious due to the water absorption of the grafted polymers, and show improved anti-fouling properties as compared to uncoated surfaces.[17,21] These coatings, however, are only a few nanometers thick and do not decrease the hardness of the underlying polymeric surface (**Figure S1**). Moreover, the grafted polymers are prone to damage

when subjected to abrasion, shearing or other mechanical loading. More recently, omniphobic surface coatings based on liquid-filled microstructures have been adopted for various materials and devices to provide non-stick, slippery, and anti-fouling properties.[22-24] While these liquid-infused coatings exhibit better mechanical robustness than the grafted polymers, they fail to provide tissue-matching properties such as mechanical compliances or high water contents.[22]

Another common strategy involves coating hydrogel layers on the surfaces of devices,[8,25-27] owing to hydrogels' favorable similarities with biological tissues in mechanical and chemical properties.[18,28-30] Given its straightforward but effective nature, interfacial bonding between the hydrogels and the polymer substrates has been one of the most widely utilized strategies to introduce soft hydrogel coatings on diverse polymer devices.[25,26,31-33] In this approach, hydrogel coatings are typically introduced to the polymer devices either in form of solid pre-formed crosslinked networks[25,27,32,33] or liquid pre-gel solutions that are then cured on the surface.[26,31] Recent advances in robust interfacial bonding between tough hydrogels and diverse polymers have enabled hydrogel coatings with improved mechanical robustness,[25,26,31] solving previously-existing issues of poor hydrogel-substrate adhesion and poor mechanical properties of common hydrogels. However, there are still unresolved challenges. Hydrogel coatings fabricated by molding or dip-coating typically result in relatively thick hydrogel layers (over 50 microns), with shapes determined by the shape of the mold or dip-coated surface used. These challenges greatly hinder the ability to conformally adapt to devices with complex surface geometries and fine features (**Figure S1**).

Here, we report a simple yet effective strategy to interpenetrate crosslinked hydrophilic polymers (namely "hydrogel skins") into the surfaces of diverse polymers including silicone rubbers, polyurethane, polyvinyl chloride, nitrile rubber, and natural rubber with arbitrary shapes. Owing to the unique combination of hydrophobic (i.e., water insoluble) initiators absorbed to the polymer

surfaces and hydrophilic (i.e., water soluble) initiators dissolved in the hydrogel pre-gel solution, the hydrogel skins can be formed *in situ* on the surfaces, conformally adapting to complex and fine geometries of the polymer substrates. The resultant hydrogel skins exhibit micron-scale tunable thickness ranging from 5 to 25-μm with tissue-like softness (Young's modulus ~ 30 kPa) and mechanical robustness. The proposed method can impart superior low-friction, antifouling, and ionically conductive surfaces to polymer devices without altering their original bulk mechanical properties or geometries. We further demonstrate applications of the hydrogel skins on various practical polymer devices with complex geometries including medical tubing, Foley catheters, cardiac pacemaker leads, and soft robots.

The essential idea and procedures for coating the hydrogels skins are illustrated in **Figure 1**. Unlike the existing methods of grafting polymer brushes or bonding separate hydrogel layers, we introduce a thin and uniform hydrogel-polymer interpenetrated layer on the outermost surface of polymer substrates. In order to achieve successful formation of the hydrogel skins, we adopt an interfacial interpenetration strategy based on a combination of surface-absorbed hydrophobic (i.e., water insoluble) initiators for the polymer substrates and hydrophilic (i.e., water soluble) initiators for the hydrogel pre-gel solutions. We first introduce a surface-bound diffusion layer of hydrophobic initiators on the pristine polymer substrates by treating their surfaces with 10 wt. % hydrophobic photo- or thermo-initiators (e.g., benzophenone, 4-methyl benzophenone, benzoyl peroxide, azobisisobutyronitrile) in organic solution (e.g., ethanol, isopropanol, acetone) via swelling-driven surface absorption.[25,34] Then, the treated polymer substrates are fully immersed into a hydrogel pre-gel solution bath composed of hydrophilic photo- or thermo- initiators (e.g., Irgacure-2959, α-ketoglutaric acid, ammonium persulfate, potassium persulfate) and hydrogel monomers (e.g., acrylamide, acrylic acid, *N*,*N*-dimethylacrylamide, *N*-vinylpyrrolidone, and hydroxyethyl

methacrylate) in aqueous solution. During the subsequent polymerization of the hydrogel pre-gel solution by UV (for photo-initiators) or heat (for thermos-initiators), the hydrophobic initiators (absorbed on the polymer substrate) serve as grafting agents for the hydrogel polymers to crosslink with the substrate polymer chains as well as oxygen scavengers to alleviate the oxygen inhibition effect.[25,35,36] Meanwhile, the hydrophilic initiators provide polymerization of hydrogel monomers into hydrogel polymers within and above the surface-bound diffusion layer of the polymer substrates. Notably, most polymer substrates are hydrophobic and swell only in organic solvents (e.g., ethanol, acetone) but not in water, allowing the surface-absorption of hydrophobic initiators dissolved in organic solvents by diffusion.[25,34] Furthermore, the insolubility of hydrophobic initiators in water prevents the diffusion of surface-absorbed hydrophobic initiators toward the aqueous hydrogel pre-gel solution, effectively limiting the reactions (i.e., polymerization, interpenetration, and grafting) within the surface-bound diffusion layer. This unique combination of selective and bounded diffusion of hydrophobic initiators enables the formation of hydrogel skins via an interfacial interpenetration process. Thereafter, the uncrosslinked hydrogel polymer solution is removed by washing with water to obtain the polymer substrates with hydrogel skins. We find that the unreacted hydrogel monomers and ungrafted polymers are mostly removed within the washing step (1 h with agitation). When the washed sample is immersed in water for the next 5 days, only negligible monomers or polymers leach out the hydrogel skin (**Figure S2**).

The unique surface-bound formation of these hydrogel skins provides highly conformal hydrogel coatings on arbitrary-shaped polymer substrates in a wide range of length scales without compromising their original geometries (**Figure 2**). At large scales, uniform hydrogel skins can be formed on the entire surface of the complex octet-truss-shaped structure made from a silicone rubber (Ecoflex 30, Smooth-On) (**Figure 2a**). At small scales, uniform hydrogel coatings can be

formed on polymer devices like a polydimethylsiloxane (PDMS; Sylgard 184, Dow Corning) microfluidic chip (minimum feature size of 20 µm) without affecting the original fine features (**Figure 2b**). Moreover, the thickness of the hydrogel skins can be easily tuned, ranging from thin coatings (~ 10 µm as shown in **Figure 2c** and **Figure S3b**) to thick coatings (~ 25 µm as shown in **Figure 2d** and **Figure S3c**) by adjusting the monomer concentration and the polymerization conditions (See **Experimental Section**). The hydrogel skins are also relatively smooth and uniform, although the thick ones may exhibit roughness due to their swelling and the subsequent appearance of surface instabilities.[37,38] The hydrogel skins also exhibit long-term stability in aqueous environment with negligible thickness changes during 7 days of soaking in water (**Figure S4**).

Since the proposed method does not rely on specific characteristics of the polymer substrate, it can be applied on a wide range of common polymers with various geometries and applications (**Table S1**). In this work, we show that hydrogel skins can be introduced to silicone rubbers (e.g., PDMS and Ecoflex), polyurethane (PU), polyvinyl chloride (PVC), nitrile rubber, and natural rubber (**Figures S5** and **S6**). Furthermore, hydrogel skins can be based on a broad range of commonly-used hydrogel monomers such as acrylic acid (AA), acrylamide (AAm), *N*,*N*-dimethylacrylamide (DMAA), *N*-vinylpyrrolidone (VP), and hydroxyethyl methacrylate (HEMA) (**Figures S5** and **S7**). The reaction conditions for diverse combinations of polymer substrates and hydrogels are summarized in **Table S2,** and the confocal microscope images of the hydrogel skins from several representative combinations are shown in **Figures S6** and **S7**.

We conduct a set of experiments to quantify the mechanical properties of the hydrogel skins (**Figure 3**). We first investigate the mechanical properties of the hydrogel skins in order to assess their ability to introduce soft tissue-like surfaces on the polymer substrates. Surface elastic modulus measurements by AFM nanoindentation of the pristine PDMS and the PDMS with AAm-based

hydrogel skin (25-μm thick) show that the presence of the hydrogel skins provide low Young's modulus (E = 27.4 ± 7.44 kPa), which is comparable to soft tissues in human body (E = 1 ~ 100 kPa)[10,15] and two orders of magnitudes lower than the pristine PDMS (E = 2.01 ± 0.128 MPa) (**Figure 3a** and **b**). Considering that the hydrogel skin is present only on the outermost 25 μm of the polymer substrate, the introduction of the hydrogel skin does not alter the bulk elastic modulus of the substrate (PDMS, 1 mm thick) (**Figure 3c**). Note that PDMS substrates are used for the measurements instead of Ecoflex substrates due to Ecoflex's Young's moduli (E = ~ 30 kPa) comparable to that of the hydrogel skins.

Furthermore, the hydrogel skin can offer a highly lubricious surface on the polymer substrate. We measure the friction coefficients of pristine Ecoflex, Ecoflex with grafted PAAm brushes (~ 100 nm thick)[39], and Ecoflex with an AAm-based hydrogel skins (25 μm thick) under varying pressures (3 ~ 160 kPa) (**Figure 3d**). The presence of the hydrogel skin provides significantly lower friction coefficients than both pristine and PAAm brushes-grafted substrates under all tested pressures. Notably, the hydrogel skin exhibits negligible increase in friction coefficient under increasing pressures while the PAAm brush grafted and the pristine Ecoflex substrates show substantial increase in their friction coefficients with the applied pressure (**Figure 3d**).

In order to investigate the mechanical robustness of the hydrogel skins, we evaluate mechanical damage of the hydrogel skins against short-term and long-term mechanical loadings. We find that the hydrogel skins show no visible damages after repeated scratching with a blunt steel needle, demonstrating adequate scratch and puncture resistance (**Figure S8** and **Video S1**). Moreover, high stretchability of the hydrogel skins allows recovery from highly-deformed state without damage such as crack or delamination (**Figure S9**). We also evaluate long-term mechanical robustness by monitoring the change in the coefficient of friction during prolonged shearing under

pressure against a steel plate (for 0 ~ 3,600 s at 3 kPa pressure) (**Figure 3e**). The hydrogel skin exhibits extraordinary robustness against long-term wear, showing negligible increase in friction coefficient over time and no visible damage even after 10 h of continuous shearing (**Figure 3f** and **Figure S10**). In contrast, the PAAm brush grafted and pristine Ecoflex substrates suffer from the gradual elevation in friction coefficient over time, largely due to wear-induced increase in surface roughness.[40] Interestingly, the friction coefficient difference between the PAAm brush-grafted and pristine Ecoflex substrates nearly disappears after 1,200 s of shearing, indicating the degradation of the grafted PAAm brushes by mechanical wear (**Figure 3f**). The superior mechanical robustness of the hydrogel skins can be attributed to the unique hydrogel-polymer interpenetrating network structure. Unlike weak and brittle grafted polymer brushes and conventional hydrogel coatings, the interpenetration of the substrate and hydrogel chains yields a significant increase in mechanical robustness, analogous to double-network tough hydrogels.[41,42]

In addition to the mechanical softness and low-friction characteristics, the hydrogel skins can provide superior antifouling property to the polymer devices. To evaluate the antifouling performance of the hydrogel skins, we quantitatively compare the density of bacteria (*Escherichia coli* (*E. coli*)) adhered to the thin and thick hydrogel skins (10 μm and 25 μm based on AAm and PDMS substrates, respectively) as well as the PAAm brush grafted and the pristine PDMS substrates (**Figure 4a**). Both thin and thick hydrogel skins exhibit much lower level of *E. coli* adhesion (~ 80 and ~ 5 counts per mm^2 for thin and thick skins, respectively) than the pristine PDMS (~ 1,300 counts per mm^2) and the PAAm brush grafted PDMS (~ 180 counts per mm^2) substrates (**Figure 4b**). The hydrogel skin's resistance to bacterial adhesion may delay the subsequent formation of biofilms and can be desirable for biomedical device coatings.[22-24]

Owing to the hydrogel skins' high water contents that can dissolve ionic species, the hydrogel skins can endow ionic conductivity to the polymer devices as well. The resultant ionically conductive hydrogel skins (or ionic skins) can serve as a thin, conformal, and transparent ionic conductor with high ionic conductivity (1 S m^{-1} with 3 M LiCl) and high stretchability (over 6 times of the original length) for various electrically-insulating polymer devices with complex shapes. Notably, the ionic skins exhibit the relation between electrical resistance and stretch as $R/R_0 = \lambda^2$ where R_0 is the resistance before deformation and R is the resistance after stretch of λ times from the original length, similar to the ionically conductive bulk hydrogels (**Figure 4c**).[43-46] To demonstrate the ionic skins on polymer devices with complex geometry, we introduce uniform DMAA-based hydrogel skins with dissolved LiCl salt (3M concentration) on the outer surface of an Ecoflex tube with diameter of 3 cm. The ionic skins provide ionic conductivity on the electrically-insulating Ecoflex tube which can light up a LED with an AC power source connected to the ionic skins (**Figure 4d**). Note that various types of salts can be used for the preparation of ionic skins such as NaCl to replace LiCl for better biocompatibility.

The broad applicability of the proposed hydrogel skins to a wide range of polymer devices enables us to explore various applications otherwise unachievable with conventional hydrogel coatings (**Table S1**). We first demonstrate applications of the hydrogel skins on various commonly-used biomedical devices such as cardiac pacemaker leads, medical tubing, and Foley catheters (**Figure 5**). Unlike other hydrogel coating approaches, the hydrogel skins are formed on all submerged polymer surfaces regardless of size or orientation, but not on non-polymeric materials (i.e. metals or ceramics) (**Figure 1**). For example, we show that thin and uniform AAm-based hydrogel skins (25 μm thick) can be successfully formed on the PU surface of long and highly flexible

cardiac pacemaker leads without affecting the metallic electrodes at the end of the pacing leads (**Figure 5a**).

While tubes are one of the most frequently used geometries in polymer devices in biomedical and clinical applications (**Table 1**), previous approaches have failed to selectively coat inner and/or outer surfaces of tube devices. In contrast, the versatility of the proposed method enables uniform hydrogel coating of both inner and outer surfaces of polymer tubes or only one of them. For example, DMAA-based hydrogel skins (25 μm thickness) can be formed on both inner and outer surfaces of a PVC tubing (**Figure 5b**) and a silicon Foley catheter (**Figure 5c**) as well as on inner surface alone for a PVC tubing (**Figure S11**). Notably, hydrogel skins can also be coated on the Foley catheter balloon and remain on the device upon inflation of the balloon, demonstrating the versatility of the proposed method (**Figure 5c**). High scalability of the fabrication process further allows the formation of hydrogel skins on long tube devices such as 1.5 m-long segment of PVC tubing in a single preparation (**Figure S11**).

As another example, existing soft robots are typically made of elastomers such as PDMS and Ecoflex in complex shapes depending on their functions and applications.[6] While hydrogel coatings can be beneficial for several soft robotic applications including medical soft robots (to decrease tissue trauma due to material rigidity and high friction)[8] and pipe leak detection soft drones (to decrease friction between robots and pipes),[47] it has been challenging to introduce hydrogel coatings on soft robots due to the complex geometries of soft robots. The advantages of the proposed hydrogel skins can open new opportunities to incorporate hydrogel coatings for these previously inaccessible soft robotic applications. As an example, we introduce a uniform AAm-based hydrogel skin to a soft drone (Ecoflex as body material) for leak detection in pipes (**Figure 6a**). We find that hydrogel skins on the soft drones can provide highly lubricious interfaces substantially

reducing fluctuations in travel speed within the pipe smaller than the drones (51 mm diameter drone in 49.25 mm diameter pipe) (**Figure 6b** and **Video S2**).

As one of the most promising routes to seamlessly integrate hydrogels' unique benefits into existing devices, hydrogel coatings on polymer devices possess a great potential in a wide range of applications. In this study, we develop a simple yet effective method to introduce thin and uniform hydrogel skins readily applicable for diverse combinations of polymers and hydrogels. We demonstrate the ability to form micron-scale thin uniform hydrogel layer on highly complex geometries without compromising fine features in the polymer substrate as small as 20 μm. Hydrogel skins boast tissue-like softness together with superior mechanical robustness, low-friction, antifouling performance, and ionic conductivity. We further show representative applications of the hydrogel skins for various polymer devices including cardiac pacemaker leads, medical tubing, Foley catheters, and pipe leak detecting soft drones, all of which are previously unachievable with conventional hydrogel coating methods. With this unprecedented capability, this work has the potential to open new avenues toward untapped opportunities for integrative hydrogel technologies and their important applications, including biomedical and clinical devices, wearable devices, and soft robotics.

Experimental Section

Materials: All chemicals were obtained from Sigma-Aldrich and used as received, unless otherwise noted. Silicone substrates were prepared by casting commercially-available silicone resins into acrylic molds. Polydimethylsiloxane (PDMS) substrates were casted by using Sylgard 184 (Dow Corning) mixture (base resin and catalyst in 10:1 weight ratio). Ecoflex 30 substrates were casted by

using Ecoflex 30 (Smooth-On) mixture (Part A and Part B in 1:1 weight ratio). Polyurethane (PU), polyvinyl chloride (PVC), nitrile rubber, and natural rubber substrates were obtained from McMaster-Carr and cleaned with isopropanol and deionized water before use. Octet truss structures were prepared by casting Ecoflex 30 mixture into a 3D printed mold. Microfluidic chips were prepared by casting Sylgard 184 mixture on a soft lithography mold (designed by collaborators in the Kamm group, MIT MechE). Cardiac pacemaker leads (PACEL Bipolar Pacing Catheter, St. Jude Medical) and Foley catheter (Bardia Foley Catheter 20Fr, C. R. Bard) were obtained from 4MD Medical Solutions. PVC tubes and balls (stainless steel, glass, polypropylene, and neoprene rubber) were obtained from McMaster-Carr and cleaned with isopropanol and deionized water before use.

Preparation of Hydrogel Skins on Diverse Polymers: The polymer substrates were first cleaned with isopropanol and deionized water followed by drying under nitrogen flow. To enhance wettability of the polymer substrates, the substrates were treated by atmospheric plasma by a plasma cleaner (PDC-001, Harrick Plasma) for 3 min. The plasma treated polymer substrates were then immersed into a hydrophobic initiator (benzophenone, 4-methylbenzophenone, benzoyl peroxide, azobisisobutyronitrile) organic solution (ethanol, isopropanol, acetone) for 3 ~ 5 min. After gently rinsing with isopropanol followed by drying under nitrogen flow, the substrates were immersed into a hydrogel monomer (acrylic acid, acrylamide, *N*,*N*-dimethylacrylamide, *N*-vinylpyrrolidone, hydroxyethyl methacrylate) aqueous solution containing hydrophilic initiator (Irgacure-2959, α-ketoglutaric acid, ammonium persulfate, potassium persulfate). To form hydrogel skins, the monomer solution bath was subjected to either UV irradiation (CL-1000, UVP) for photo-initiators or 80 ºC oven for 30 ~ 90 min. After formation of hydrogel skins, unreacted regents were thoroughly

rinsed with a large amount of deionized water for 24 h. Typical protocols for various combinations of polymers and hydrogels is summarized in **Table S2**.

Imaging of Hydrogel Skins: Due to optical transparency of hydrogel skins, different dyes were utilized to facilitate imaging and characterization of hydrogel skins. For macroscale photographs, samples were immersed in 2 % aqueous green or blue food dye (McCormick) solution for 1 min to colorize hydrogel skins. The colorized samples were lightly rinsed with flowing water to remove excess dye solution from the surface before imaging by a digital camera (D7000, Nikon). For confocal microscope images, a hydrophobic Nile red dye ($\lambda_{emission}$ ~ 600 nm) was added to Sylgard 184 mixture prior to casting PDMS substrate to allow visualization of the polymer substrate while hydrogel skins were immersed in an aqueous fluorescein solution ($\lambda_{emission}$ ~ 510 nm) to visualization of hydrogel skins. All confocal microscope images were obtained by an upright confocal microscope (SP8, Leica) using the z-stack acquisition program (slice thickness ~ 1 μm). For cross-section imaging, samples were immersed in 2 % aqueous blue food dye (McCormick) solution for 1 min to provide better contract to hydrogel skins. The colorized samples were lightly rinsed with flowing water to remove excess dye solution from the surface before imaging by a compound microscope (Eclipse LV100ND, Nikon). For high-resolution surface imaging, samples were sputtered with gold and imaged by a scanning electron microscope (SEM; 6010LA, JEOL).

Leaching Tests: Hydrogel skins based on acrylic acid were formed on PDMS substrates and cut into square samples (4 cm × 4 cm) before leaching tests. Each square sample was placed in 100 mL deionized water in separate containers. PDMS substrates without hydrogel skin were also placed in

deionized water as control. The amount of acrylic acid monomer and polymer leached into the solution was monitored based on absorbance at 285 nm (reference wavelength 350 nm) at various time points by a UV-Vis spectrophotometer (BioMate 3S, Thermo Scientific).

Mechanical Characterizations: Young's moduli of samples were obtained by fitting force vs. indentation depth curve with a JKR model.[48] Nanoindentation tests were performed by an atomic force microscope (MFP-3D, Asylum Research) with 50 nm indentation depth. To avoid drying of hydrogel skins, nanoindentation tests were done within water bath equipped in the atomic force microscope. Uniaxial tensile tests were performed by a mechanical tester (Z2.5, Zwick/Roell) at strain rate of 0.1 s^{-1}. Scratching tests of hydrogel skins were performed by using a blunt-tip 26-gauge stainless steel needle (Nordson EFD) under the compound microscope.

Friction Coefficient Measurements: Friction coefficients of samples were measured by a rotational rheometer (AR-G2, TA Instruments) in normal force control mode with 20 mm steel parallel plate fixtures. The friction coefficients were obtained by following the previously reported protocol.[26] Briefly, pristine Ecoflex 30, Ecoflex 30 grafted with PAAm brush,[19] and Ecoflex 30 with thick hydrogel skins (25 μm based on AAm) were prepared and cut into square samples (4 cm × 4 cm). Then, each sample was loaded into the rheometer and a set of normal pressures (3 ~ 160 kPa) was applied to the sample immersed in deionized water bath at steady-state shear rate of 0.5 s^{-1}.

Antifouling Tests: An engineered *Escherichia coli* (*E. coli*) strain that constitutively expresses green fluorescent protein (GFP) was prepared by following the previously reported protocol,[32,49] and cultured in Luria-Bertani broth (LB broth) overnight at 37 °C. 1 µL of bacteria culture diluted in 1 mL of fresh LB broth was placed on samples (1 cm × 1 cm) and incubated for 24 h at 37 °C. After the incubation, the samples were taken out and rinsed with phosphate buffered saline (PBS) to remove the free-floating bacteria, and imaged with a fluorescence microscope (Eclipse LV100ND, Nikon). The number of adhered *E. coli* on the samples per unit area (mm^2) were counted by Image J.

Preparation and Characterizations of Ionic Skins: To introduce ionic conductivity to the hydrogel skins, Ecoflex 30 sheets or tubes were introduced with hydrogel skins (25 µm based on DMAA), and then immersed in the 3M LiCl solution for 1 h. To introduce a pristine Ecoflex area between two ionic skins, a Kapton tape was applied on the Ecoflex tube during the hydrogel skin formation. To light up a LED on the ionic skins, each side of the ionic skins were connected to an AC power source (5 V peak-to-peak voltage at 1 kHz sine input). The electrical properties of the ionic skins were measured using the four-point method following the previously reported protocols.[25,50]

Pipe Soft Drone Tests: Pipe leak detecting soft drones were prepared by following the previously reported protocol[47] and introduced with hydrogel skins (25 µm based on AAm). The soft drones travel tests were performed by using a clear PVC pipe (49.25 mm diameter) with 20 kPa applied water pressure. The speed of drone travel inside the pipe was obtained by analyzing the recorded footage of tests (**Video S2**).

Supporting Information

Supporting Information is available from the Wiley Online Library or from the author.

Acknowledgements

Y.Y., H.Y., and G.A.P. contributed equally to this work. H.Y., Y.Y., G.A.P., and X.Z. conceived the idea and designed the study. Y.Y., H.Y., and G.A.P. prepared samples and conducted the experiments. Y.W. and K.Y.-T. performed and analyzed the pipe soft robot experiments. Y.Y. and X.L. performed the antifouling experiments. H.Y., G.A.P., Y.Y., and X.Z. analyzed and interpreted the result, and wrote the manuscript. The authors thank to Dr. Alan F. Schwartzman in MIT DMSE NanoMechanical Technology Laboratory for his help with AFM nanoindentation experiments. This work is supported by National Science Foundation (CMMI-1661627), Office of Naval Research (N00014-17-1-2920), and U.S. Army Research Office through the Institute for Soldier Nanotechnologies at MIT (W911NF-13-D-0001). H.Y. acknowledges the financial support from Samsung Scholarship.

Received: ((will be filled in by the editorial staff))
Revised: ((will be filled in by the editorial staff))
Published online: ((will be filled in by the editorial staff))

References

1 A. J. T. Teo, A. Mishra, I. Park, Y.-J. Kim, W.-T. Park, Y.-J. Yoon*, ACS Biomater. Sci. Eng.* **2016**, *2*, 454-472.

2 Y. Onuki, U. Bhardwaj, F. Papadimitrakopoulos, D. J. Burgess, *J. Diabetes Sci. Technol.* **2008**, *2*, 1003-1015.

3 Ž. Marjanović-Balaban, D. Jelić, *Polymeric Biomaterials in Clinical Practice* **2018**, 101-117.

4 S. Haeberle, R. Zengerle, *Lab Chip* **2007**, *7*, 1094-1110.

5 F. Ilievski, A. D. Mazzeo, R. F. Shepherd, X. Chen, G. M. Whitesides, *Angew. Chem. Int. Ed.* **2011**, *123*, 1930-1935.

6 D. Rus, M. T. Tolley, *Nature* **2015**, *521*, 467.

7 E. Bouza, M. Guembe, P. Munoz, *Int. J. Antimicrob. Agents.* **2010**, *36*, S22-25.

8 E. T. Roche, M. A. Horvath, I. Wamala, A. Alazmani, S.-E. Song, W. Whyte, Z. Machaidze, C. J. Payne, J. C. Weaver, G. Fishbein, J. Kuebler, N. V. Vasilyev, D. J. Mooney, F. A. Pigula, C. J. Walsh, *Sci. Transl. Med.* **2017**, *9*, eaaf3925.

9 W. Whyte, E. T. Roche, C. E. Varela, K. Mendez, S. Islam, H. O'Neill, F. Weafer, R. N. Shirazi, J. C. Weaver, N. V. Vasilyev, P. E. McHugh, B. Murphy, G. P. Duffy, C. J. Walxh, D. J. Mooney, *Nat. Biomed. Eng.* **2018**, *2*, 416.

10 J.-W. Jeong, G. Shin, S. I. Park, K. J. Yu, L, Xu, J. A. Rogers, *Neuron* **2015**, *86*, 175-186.

11 R. Feiner, T. Dvir, *Nat. Rev. Mater.* **2017**, *3*, 17076.

12 J. M. Anderson, A. Rodriguez, D. T. Chang, *Semin. Immunol.* **2008**, *20*, 86-100.

13 I. Dimarakis, S. M. Rehman, G. Asimakopoulos, *Biomaterials and Devices for the Circulatory System* **2010**, 3-23.

14 W. M. Grill, S. E. Norman, R. V. Bellamkonda, *Annu. Rev. Biomed. Eng.* **2009**, *11*, 1-24.

15 S. P. Lacour, G. Courtine, J. Guck, *Nat. Rev. Mater.* **2016**, *1*, 16063.

16 J. Rivnay, H. Wang, L. Fenno, K. Deisseroth, G. G. Malliaras, *Sci. Adv.* **2017**, *3*, e1601649.

17 C. Desrousseaux, V. Sautou, S. Descamps, O. Traore, *J. Hosp. Infect.* **2013**, *85*, 87-93.

18 K. Y. Lee, D. J. Mooney, *Chem. Rev.* **2001**, *101*, 1869-1880.

19 A. Parvin, H. Mirzadeh, M. Khorasani, *J. Appl. Polym. Sci.* **2008**, *107*, 2343-2349.

20 M. R. Nejadnik, H. C. van der Mei, W. Norde, H. J. Busscher, *Biomaterials* **2008**, *29*, 4117-4121.

21 J. L. Harding, M. M. Reynolds, *Trends Biotechnol.* **2014**, *32*, 140-146.

22 T.-S. Wong, S. H. Kang, S. K. Y. Tang, E. J. Smythe, B. D. Hatton, A. Grinthal. J. Aizenberg, *Nature* **2011**, *477*, 443-447.

23 A. K. Epstein, T.-S. Wong, R. A. Belisle, E. M. Boggs, J. Aizenberg, *Proc. Natl. Acad. Sci. USA* **2012**, *109*, 13182-13187.

24 D. C. Leslie, A. Waterhouse, J. B. Berthet, T. M. Valentin, A. L .Watters, A. Jain, P. Kim, B. D. Hatton, A. Nedder, K .Donovan, E. H. Super, C. Howell, C. P. Johnson, T. L. Vu, D. E. Bolgen, S. Rifai, A. R. hansen, M. Aizenberg, M. Super, J. Aizenberg, D. E. Ingber, *Nat. Biotechnol.* **2014**, *32*, 1134-1140.

25 H. Yuk, T. Zhang, G. A. Parada, X. Liu, X. Zhao, *Nat. Commun.* **2016**, *7*, 12028.

26 G. A. Parada, H. Yuk, X. Liu, A. J. Hsieh, X. Zhao, *Adv. Healthc. Mater.* **2017**, *6*, 1700520.

27 D. Wirthl, R. Pichler, M. Drack, G. Kettlguber, R. Moser, R. Gerstmayr, F. hartmann, E. Bradt, R. Kaltseis, C. M. Siket, S. E. Schausberger, S. Hild, S. Bauer, M. Kaltenbrunner, *Sci. Adv.* **2017**, *3*, e1700053.

28 N. A. Peppas, J. Z. Hilt, A. Khademhosseini, R. Langer, *Adv. Mat.* **2006**, *18*, 1345-1360.

29 A. S. Hoffman, *Adv. Drug Deliv. Rev.* **2012**, *64*, 18-23.

30 E. Caló, V. V. Khutoryanskiy, *Eur. Polym. J.* **2015**, *65*, 252-267.

31 H. Yuk, T. Zhang, S. Lin, G. A. Parada, X. Zhao, *Nat. Mater.* **2016**, *15*, 190-196.

32 X. Liu, T.-C. Tang, E. Tham, H. Yuk, S. Lin, T. K. Lu, X. Zhao, *Proc. Natl. Acad. Sci. USA* **2017**, *114*, 2200-2205.

33 Q. Liu, G. Nian, C. Yang, S. Qu, Z. Suo, *Nat. Commun.* **2018**, *9*, 846.

34 M. H. Schneider, Y. Tran, P. Tabeling, *Langmuir* **2011**, *27*, 1232-1240.

35 G. Dorman, G. D. Prestwich, *Biochemistry* **1994**, *33*, 5661-5673.

36 W. Yang, B. Rånby, *Macromolecules* **1996**, *29*, 3308-3310.

37 K. Saha, J. Kim, E. Irwin, J. Yoon, F. Momin, V. Trujillo, D. V. Schaffer, K. E. Healy, R. c. Hayward, *Biophys. J.* **2010**, *99*, L94-L96.

38 M. K. Kang, R. Huang, *J. Mech. Phys. Solids* **2010**, *58*, 1582-1598.

39 Y. Wang, H.-H. Lai, M. Bachman, C. E. Sims, G. P. Li, N. L. Allbritton, *Anal. Chem.* **2005**, *77*, 7539-7546.

40 M. Barquins, *Wear and Friction of Elastomers* **1992**.

41 J.-Y. Sun, X. Zhao, W. R. K. Illeperuma, O. Chaudhuri, K. H. Oh, D. J. Mooney, J. J. Vlassak, Z. Suo, *Nature* **2012**, *489*, 133-136.

42 X. Zhao, *Soft Matter* **2014**, *10*, 672-687.

43 C. Keplinger, J.-Y. Sun, C. C. Foo, P. Rothemund, G. M. Whitesides, Z. Suo, *Science* **2013**, *341*, 984-987.

44 J.-Y. Sun, C. Keplinger, G. M. Whitesides, Z. Suo, *Adv. Mater.* **2014**, *26*, 7608-7614.

45 C.-C. Kim, H.-H. Lee, K. H. Oh, K. H. J.-Y. Sun, *Science* **2016**, *353*, 682-687.

46 M. S. Sarwar, Y. Dobashi, C. Preston, J. K. M. Wyss, S. Mirabbasi, J. D. Wyndham, *Sci. Adv.* **2017**, *3*, e1602200.

47 Y. Wu, K. Kim, M. F. Henry, K. Youcef-Toumi, *2017 IEEE/RSJ International Conference on. Intelligent Robots and Systems (IROS)* 6075-6082.

48 K. L. Johnson, K. Kendall, A. Roberts, *Proc. R. Soc. Lond. A* **1971**, *324*, 301-313.

49 X. Liu, H. Yuk, S. Lin, G. A. Parada, T.-C. Tang, E. Tham, C. de la Fuente-Nunez, T. K. Lu, X. Zhao, *Adv. Mater.* **2018**, *30*, 1704821.

50 C. H. Yang, B. Chen, J. J. Lu, J. H. Yang, J. Zhou, Y. M. Chen, Z. Suo, *Extreme Mech. Lett.* **2015**, *3*, 59-65.

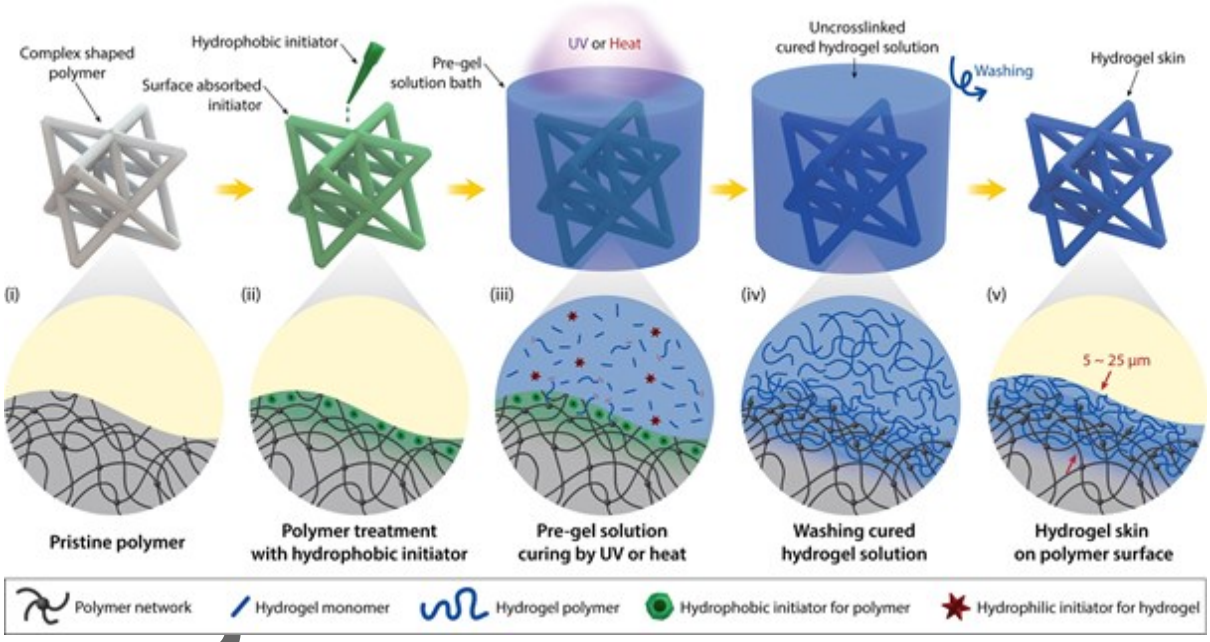

Figure 1. Schematic illustration of hydrogel skin preparation procedures. First, polymer substrates are treated with a hydrophobic initiator organic solution. Then, the treated polymer substrates are immersed into a hydrogel monomer aqueous solution containing hydrophilic initiators. After curing and washing the hydrogel monomer solution, uniform and thin hydrogel skins are formed on the polymer surface by the surface-bound formation of hydrogel-polymer interpenetrating networks.

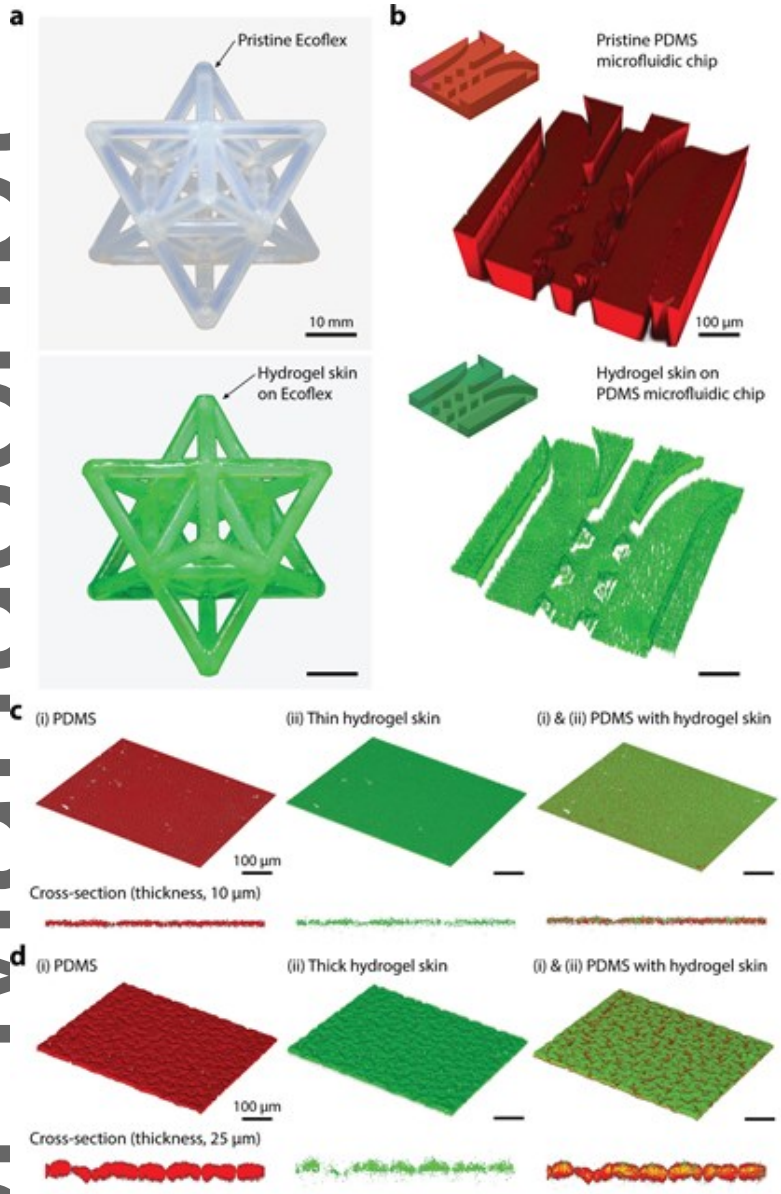

Figure 2. Hydrogel skins on diverse arbitrary shaped polymers. a) Octet truss structures made of Ecoflex with and without hydrogel skins. Hydrogel skins are colorized by green food dye. b) Confocal microscope images of PDMS microfluidic chips with and without hydrogel skins. PDMS and hydrogel skins are colorized by Nile red and fluorescein, respectively. c,d) Confocal microscope images of (c) thin and (d) thick hydrogel skins on the PDMS substrates to illustrate the uniformity and tunable thickness of hydrogel skins. PDMS and hydrogel skins are colorized by Nile red and fluorescein, respectively.

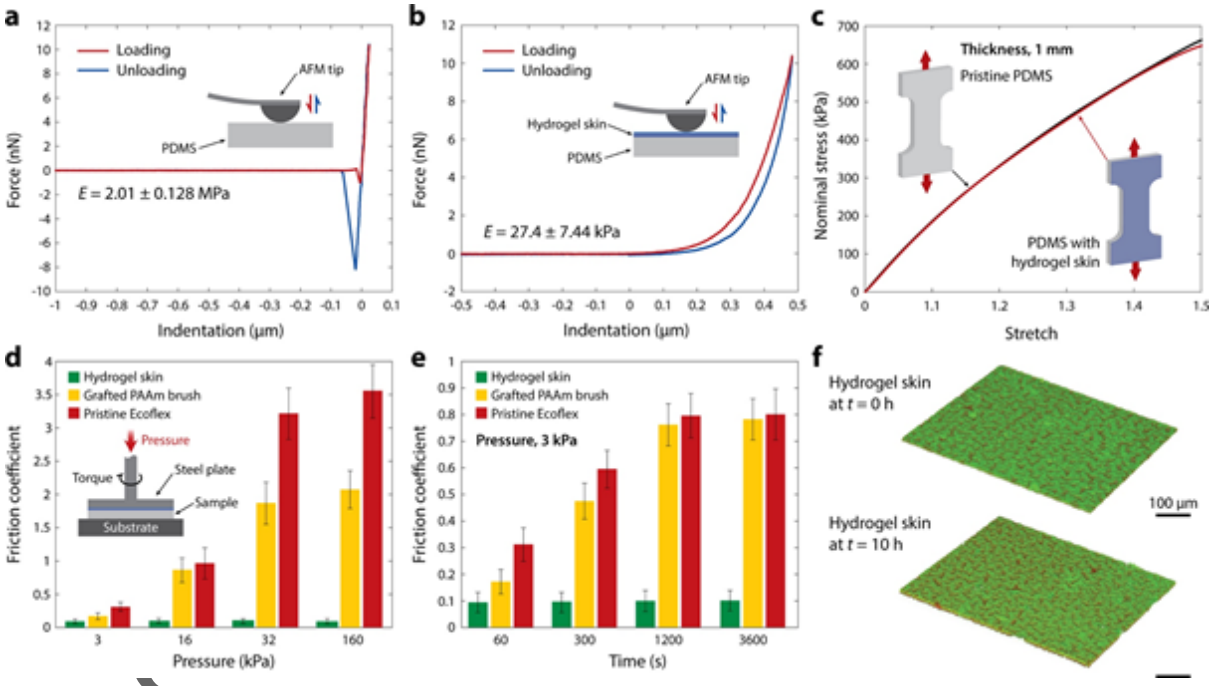

Figure 3. Mechanical properties of hydrogel skins. a,b) Nanoindentation curves for PDMS substrates (a) without and (b) with hydrogel skins. Values for Young's modulus indicate the average and the standard deviation (n = 20 repeats). c) Nominal stress vs. stretch curves for PDMS substrates with and without hydrogel skins. d) Friction coefficients of pristine Ecoflex, Ecoflex grafted with PAAm brush, and Ecoflex with hydrogel skins under different normal pressures (n = 3 repeats). e) Friction coefficients of pristine Ecoflex, Ecoflex grafted with PAAm brush, and Ecoflex 30 with hydrogel skins at 3 kPa normal pressure after the extended periods of friction testing (n = 3 repeats). f) Confocal microscope images of hydrogel skins before and after 10 h friction testing. Ecoflex and hydrogel skins are colorized by Nile red and fluorescein, respectively.

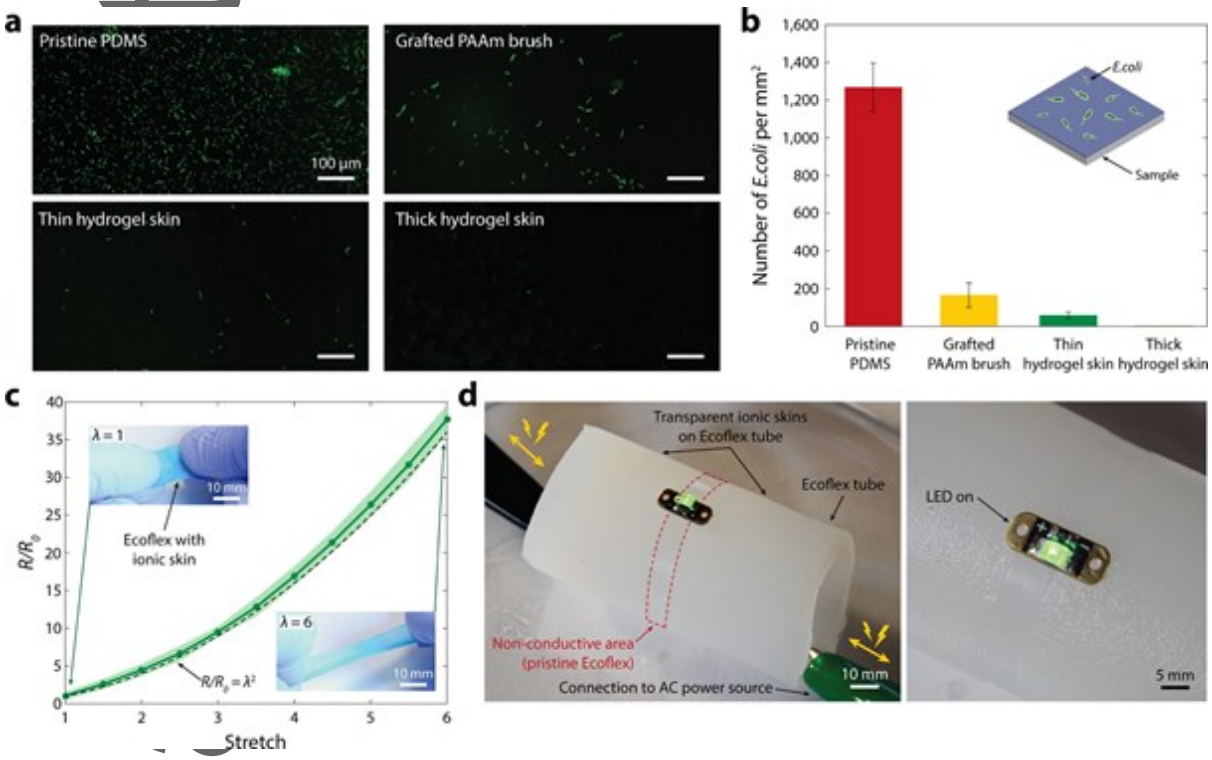

Figure 4. Antifouling and ionically conductive properties of hydrogel skins. a) Fluorescent microscope images of *E. coli* adhered to pristine PDMS, PDMS grafted with PAAm brush, and PDMS with hydrogel skins after 24 h incubation. b) The number of adhered *E. coli* per unit area (mm^2) for each substrate (n = 3 repeats). c) Normalized electrical resistance vs. stretch for Ecoflex sheet with ionic skins. Hydrogel skins are colorized by blue food dye. d) The ionic skins on an Ecoflex tube connected with an AC power source can light up a LED.

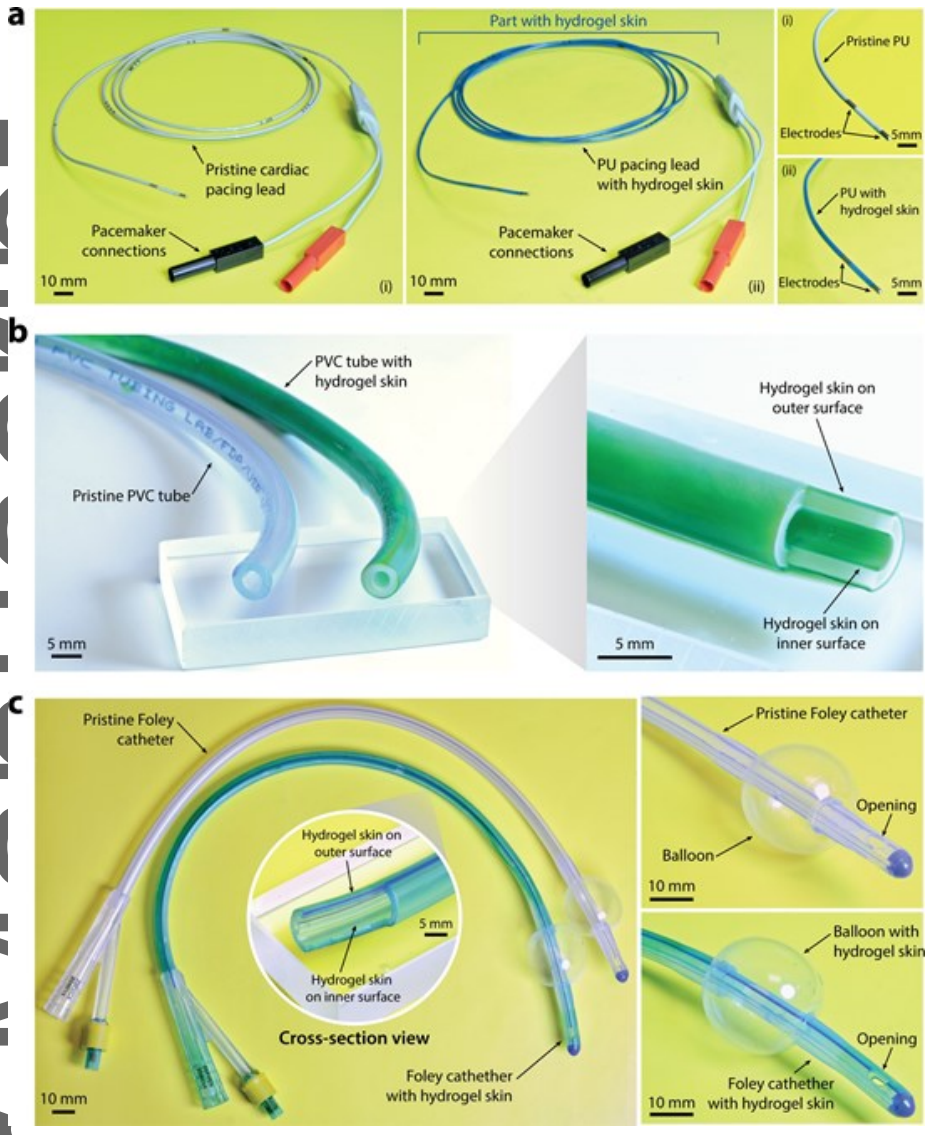

Figure 5. Applications of hydrogel skins on medical devices. a) Polyurethane (PU) pacemaker leads with and without hydrogel skins on outer surface. Hydrogel skins are colorized by blue food dye. b) PVC tubing with and without hydrogel skins on both inner and outer surfaces. Hydrogel skins are colorized by green food dye. c) Silicone Foley catheters with and without hydrogel skins on both inner and outer surfaces. Hydrogel skins are intact even after inflation of balloon. Hydrogel skins are colorized by green food dye.

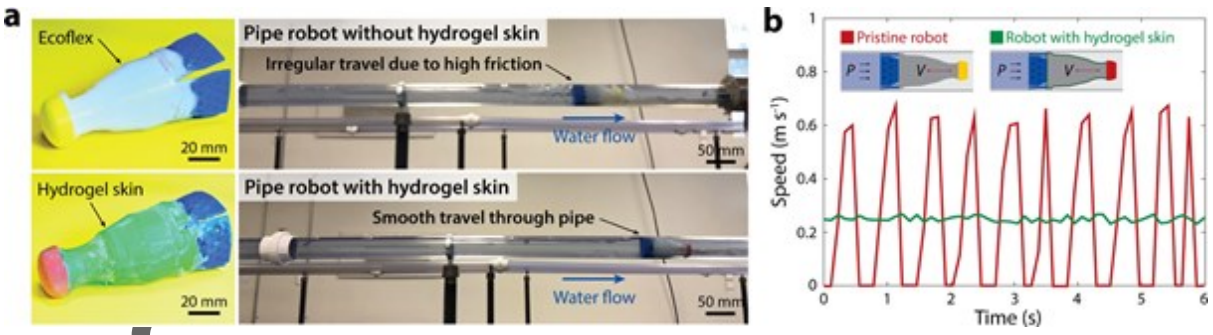

Figure 6. Applications of hydrogel skins on soft robots. a) Pipe leak detection soft drones and their travel through PVC pipes with and without hydrogel skins. Hydrogel skins are colorized by green food dye. b) The travel speed of the soft drones inside the PVC pipes with and without hydrogel skins. The drone with hydrogel skins show much smoother travel than the pristine drone.

Multifunctional hydrogel skins are reported by interpenetrating hydrophilic polymers into the surfaces of diverse polymers with arbitrary shapes to provide soft, low-friction, hydrophilic, antifouling, and ionically conductive surfaces. This new strategy not only addresses challenges for existing methods but also enables unprecedented applications including hydrogel-coated complex medical devices and soft robots on massive scales.

Keyword: Hydrogels, Polymer devices, Coatings, Low friction, Antifouling, Biomedical devices

Yan Yu, Hyunwoo Yuk, German A. Parada, You Wu, Xinyue Liu, Christoph S. Nabzdyk, Kamal Youcef-Toumi, Jianfeng Zang, Xuanhe Zhao

Multifunctional "Hydrogel Skins" on Diverse Polymers with Arbitrary Shapes